

# Energy Detection Algorithm for Spectrum Sensing Using Three Consecutive Sensing Events

Calin Vladeanu, *Member, IEEE*, Cosmina-Valentina Nastase and Alexandru Martian, *Member, IEEE*

**Abstract**—An energy detection (ED) algorithm, which takes into consideration three consecutive sensing events, is introduced in this letter. This algorithm, named three-event ED (3EED), takes the decision in one sensing event, considering also the event immediately before and the one immediately after it. We design the proposed algorithm to exploit the knowledge of the primary user (PU) activity duty cycle value for tracking the changes of the PU state and we prove that 3EED becomes independent of the PU model parameters for a low duty cycle. In this letter, we demonstrate that 3EED has better detection performance compared to the conventional ED (CED) algorithm, providing a correct detection probability (CDP) gain of more than 7% for a false-alarm probability (FAP) of 0.1. Also, we compare 3EED with other algorithms in terms of detection performance and complexity.

**Index Terms**—Energy detection, spectrum sensing, cognitive radio, PU activity duty cycle.

## I. INTRODUCTION

**D**URING the last decades, the cognitive radio (CR) schemes were rapidly emerging as spectrum efficient solutions for wireless communications. Measurement campaigns revealed that a large amount of spectrum is inefficiently used by the licensed or primary users (PUs) [1]. Therefore, the non-licensed or secondary users (SUs) must employ a spectrum sensing technique to detect the spectral holes of PU. In most applications, the classical energy detection (CED) is used [2]. An improved ED (IED) algorithm was proposed in [3], which outperforms CED by taking the decision based on an energy value averaged over more sensing events.

In the previously mentioned algorithms, the energy detection is performed assuming no prior knowledge of the PU activity model. Recently, many works pointed out that PU's activity follows a hidden Markov model (HMM) and its application to CR systems has a great impact on their performances [4]–[8]. We propose here a new algorithm, named three-event ED (3EED) that is designed to exploit the knowledge of the average duty cycle value for the PU activity model. In fact, 3EED uses three consecutive sensing events, i.e., it takes the decision in one sensing event, considering also the event immediately before and the one immediately after it. As it will be demonstrated later, when the PU's average duty cycle value is low, the threshold expression for 3EED becomes independent of the parameters of the PU activity model. For low duty cycle values, the analysis shows that 3EED outperforms CED and performs similar to IED.

C. Vladeanu, C.-V. Nastase, and A. Martian are with Telecommunications Department, Polytechnic University of Bucharest, 1-3 Iuliu Maniu, Bucharest, Romania. Emails: calin@comm.pub.ro, {cosmina,martian}@radio.pub.ro.

Manuscript received April 19, 2005; revised September 17, 2014.

The paper is structured as follows. In Section II, we introduce the 3EED algorithm. In Section III, we estimate analytically the average false-alarm probability (FAP) and correct detection probability (CDP) of the new algorithm. Section IV includes the analyses of the receiver operating characteristics (ROCs), the offset between target and experienced FAP, and the computational complexity, for 3EED and other algorithms. Finally, the conclusions are drawn in Section V.

## II. PRESENTATION OF THE NEW 3EED ALGORITHM

Several works considered a two-state HMM for the PU activity, which includes the “idle” state (PU does not transmit) and the “busy” state (PU transmits) [4], [6], [8]. In reality, in any licensed system, the PU transmits in bursts. Let us assume that the sensing time slot (i.e., the number of PU signal samples used to compute the energy) is small enough to have an average number of  $B$  sensing events (or slots) per each “busy” period. Also, we will assume that the “idle” period includes  $T - B$  slots. Here,  $T$  denotes the total time of the transmission cycle. Considering all the above, the ED algorithm can operate only on three consecutive sensing events, because for this PU activity model, the current event is more related to the preceding event and to the next event, than to the rest of events. Next, we will introduce the 3EED algorithm that estimates the energy values for three consecutive sensing slots and it takes the decision for the middle one. Let us denote by  $E_i$  the value of the energy estimated in the current sensing slot  $i$  and by  $\lambda$  the detection threshold. Hence, the correct PU signal detection in the sensing slot  $i$  assumes to set the decision variable  $q_i = 1$  if  $E_i > \lambda$ , for the “busy” state ( $H_1$  hypothesis, i.e., the signal received by SU includes the channel noise and the PU signal) and  $q_i = 0$  if  $E_i \leq \lambda$ , for the “idle” state ( $H_0$  hypothesis, i.e., the signal received by SU includes only the channel noise). First, 3EED estimates the energy in three consecutive slots,  $E_{i-1}, E_i, E_{i+1}$ . In order to decide for the current event, the  $E_i$  value is checked first. The PU is detected as present or the channel as “busy” if  $E_i$  exceeds  $\lambda$ . However, if the value of  $E_i$  is lower than the threshold, an additional check is performed for the energy in the preceding sensing slot,  $E_{i-1}$ . Again, if the energy value  $E_{i-1}$  is larger than the threshold, the PU is detected as present. Only when the detections in the sensing slots  $i$  and  $i - 1$  could not find the PU as present, a final check is performed for the next slot  $i + 1$ . Finally, the PU is detected as present if  $E_{i+1}$  exceeds the threshold. In conclusion, the 3EED algorithm checks the energy value in three consecutive sensing slots and detects the PU signal as present in the current slot  $i$  ( $q_i = 1$ ) if the energy exceeds the threshold in any of these three intervals, i.e.,  $i, i - 1$ , and

$i + 1$ , respectively. Otherwise, if the PU signal could not be found in any of these three intervals, the PU is considered as absent ( $q_i = 0$ ). One can notice that the 3EED algorithm introduces a processing delay of maximum one sensing slot. For a better detection of the changes of the PU's state, the sensing slot can be shrunk. Hence, the delay introduced by 3EED becomes negligible, but the computational effort will also increase. For 3EED and other algorithms, the complexity is analysed in subsection IV-C.

### III. THEORETICAL PERFORMANCES OF 3EED

Let us consider the PU activity model from Section II, where  $B$  and  $T$  are known. Then, the FAP of the PU signal detection using 3EED can be calculated by:

$$\begin{aligned} P_{fa}^{3EED} &= P(E_i > \lambda|H_0) + P(E_i \leq \lambda|H_0) \cdot \\ &[p_{00x} \cdot P(E_{i-1} > \lambda|H_0) + p_{10x} \cdot P(E_{i-1} > \lambda|H_1)] + \\ &P(E_i \leq \lambda|H_0) \cdot \\ &[p_{00x} \cdot P(E_{i-1} \leq \lambda|H_0) + p_{10x} \cdot P(E_{i-1} \leq \lambda|H_1)] \cdot \\ &[p_{x00} \cdot P(E_{i+1} > \lambda|H_0) + p_{x01} \cdot P(E_{i+1} > \lambda|H_1)] \end{aligned} \quad (1)$$

where  $H_0$  and  $H_1$  were defined in Section II. For  $B \geq 3$  and  $T - B \geq 2$ , the following expressions can be derived for the probabilities of the three consecutive events with a signal absence in the middle, denoted as  $p_{q_{i-1}, 0, q_{i+1}}$  in (1):

$$\begin{aligned} p_{00x} &= p_{000} + p_{001} = \frac{T-B-2}{T-B} + \frac{1}{T-B} = \frac{T-B-1}{T-B}; \\ p_{10x} &= p_{100} = \frac{1}{T-B}; p_{x01} = p_{001} = \frac{1}{T-B}; \\ p_{x00} &= p_{100} + p_{000} = \frac{1}{T-B} + \frac{T-B-2}{T-B} = \frac{T-B-1}{T-B}. \end{aligned} \quad (2)$$

where the subscript  $x$  denotes that any value may be detected, i.e.,  $q_i = x \in \{0, 1\}$ . The sequence probability values in (2) are obtained assuming that the average number of  $T - B$  "idle" slots is known. Hence, the total number of sequences with three consecutive events having a signal absence in the middle is  $T - B$ . Among these, there are only two sequences including a "busy" slot, i.e.,  $\{q_{i-1} = 1, q_i = 0, q_{i+1} = 0\}$  and  $\{q_{i-1} = 0, q_i = 0, q_{i+1} = 1\}$ , which happen at the beginning and, respectively, at the end of the "idle" period. All the other  $T - B - 2$  sequences include three consecutive "idle" slots.

Considering that each energy detection event is an independent CED problem and using (2), (1) can be rewritten as:

$$\begin{aligned} P_{fa}^{3EED} &= P_{fa}^{CED} + \left(1 - P_{fa}^{CED}\right) \cdot \\ &\left(\frac{T-B-1}{T-B} \cdot P_{fa}^{CED} + \frac{1}{T-B} \cdot P_d^{CED}\right) \cdot \\ &\left[1 + \frac{T-B-1}{T-B} \left(1 - P_{fa}^{CED}\right) + \frac{1}{T-B} \cdot \left(1 - P_d^{CED}\right)\right] \end{aligned} \quad (3)$$

In a similar way, the CDP for 3EED can be estimated by:

$$\begin{aligned} P_d^{3EED} &= P(E_i > \lambda|H_1) + P(E_i \leq \lambda|H_1) \cdot \\ &[p_{01x} \cdot P(E_{i-1} > \lambda|H_0) + p_{11x} \cdot P(E_{i-1} > \lambda|H_1)] + \\ &P(E_i \leq \lambda|H_1) \cdot \\ &[p_{01x} \cdot P(E_{i-1} \leq \lambda|H_0) + p_{11x} \cdot P(E_{i-1} \leq \lambda|H_1)] \cdot \\ &[p_{x10} \cdot P(E_{i+1} > \lambda|H_0) + p_{x11} \cdot P(E_{i+1} > \lambda|H_1)] \end{aligned} \quad (4)$$

For  $B \geq 3$ , as in (2), the probabilities of three events with a signal presence event in the middle are given by:

$$\begin{aligned} p_{01x} &= p_{011} = \frac{1}{B}; p_{x10} = p_{110} = \frac{1}{B}; \\ p_{11x} &= p_{111} + p_{110} = \frac{B-2}{B} + \frac{1}{B} = \frac{B-1}{B}; \\ p_{x11} &= p_{011} + p_{111} = \frac{1}{B} + \frac{B-2}{B} = \frac{B-1}{B}. \end{aligned} \quad (5)$$

Similarly, considering the expressions in (5), the CDP in (4) can be rewritten as a function of FAP and CDP of CED:

$$\begin{aligned} P_d^{3EED} &= P_d^{CED} + \left(1 - P_d^{CED}\right) \cdot \\ &\left(\frac{1}{B} \cdot P_{fa}^{CED} + \frac{B-1}{B} \cdot P_d^{CED}\right) \cdot \\ &\left[1 + \frac{1}{B} \left(1 - P_{fa}^{CED}\right) + \frac{B-1}{B} \cdot \left(1 - P_d^{CED}\right)\right] \end{aligned} \quad (6)$$

The CDP of 3EED from (6) depends only on  $B$ , while its FAP from (3) depends both on  $B$  and  $T$ . For  $T - B \rightarrow \infty$  (PU is not active; this is the best scenario for CR), the FAP of the 3EED algorithm from (3) can be rewritten as:

$$P_{fa, T-B \rightarrow \infty}^{3EED} = 3P_{fa}^{CED} - 3\left(P_{fa}^{CED}\right)^2 + \left(P_{fa}^{CED}\right)^3 \quad (7)$$

In this ideal case, the FAP of 3EED depends only on the FAP of CED. This allows us to determine an exact expression for the threshold  $\lambda$ , considering this ideal value of  $P_{fa}^{3EED}$  as the target FAP. The only real solution (the equation's discriminant (1) is negative:  $\Delta = -27(1 - P_{fa}^{CED})^2 < 0$ ) for the cubic equation in (7), having  $P_{fa}^{CED}$  as variable, is given by:

$$P_{fa}^{CED} = 1 + \sqrt[3]{P_{fa, target}^{3EED} - 1} \quad (8)$$

Using the well-known expression of the  $P_{fa}^{CED}$  [3], we can derive the value of the threshold  $\lambda$  from (8) as following:

$$\lambda = \left[Q^{-1} \left(1 + \sqrt[3]{P_{fa, target}^{3EED} - 1}\right) \sqrt{2N} + N\right] \sigma_w^2 \quad (9)$$

where  $N$  is the number of signal samples from a sensing slot.

It is very important to remark that, even if 3EED was defined in the context of a PU activity with a  $B/T$  duty cycle, the value of  $\lambda$  given by (8) does not depend on the activity model's parameters, i.e.,  $B$  and  $T$ . Therefore, in case of an almost "idle" system, 3EED becomes independent of the PU activity. In the next section, we will show that this independency is reached for practical values of the duty cycle.

### IV. PERFORMANCE ANALYSIS

In this section, we analyse the ROC plots, the offset between the target and the experienced values for FAP, and the computational complexity, for the studied ED algorithms.

#### A. Simulated versus theoretical ROC analysis

In this subsection, the ROC plots (represented as CDP versus FAP) for the 3EED algorithm will be compared with the corresponding plots of some reference ED algorithms.

In [3], the authors estimated the performance of IED considering that the receiver may found  $M$  "busy" sensing slots out of a window of  $L$  slots. IED averages the energy values from  $L$  preceding sensing slots to improve the decision in the current sensing slot. Also, the work in [3] does not consider a PU activity model and therefore, the receiver parameters  $M$  and  $L$  are not related to the transmitter parameters  $B$  and  $T$ .

In order to have a fair comparison in terms of sensing time, we consider two modified versions of CED that make decisions independently in three sensing slots and combine these decisions using the logical "OR" and "AND" rules, respectively, as in a cooperative scheme. We denote these modified cooperative CED (CCED) algorithms as 3-OR-CCED and 3-AND-CCED.

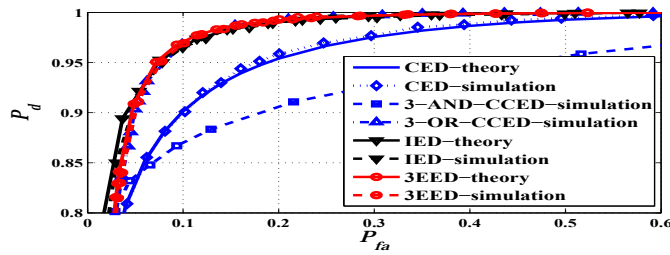


Fig. 1. ROC curves for ED algorithms with  $B = 10$  and  $T = 50$ .

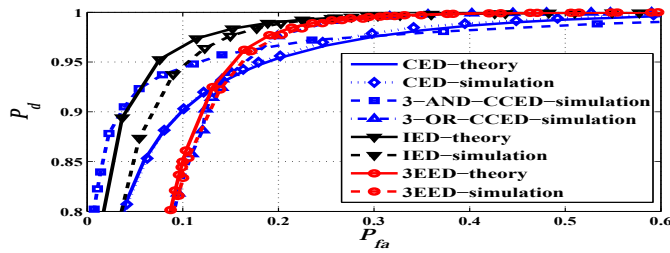


Fig. 2. ROC curves for ED algorithms with  $B = 40$  and  $T = 50$ .

Also, for a fair comparison, we consider that IED computes the average energy for  $L = 3$  sensing events. Therefore, the sensing time of CCED, IED, and 3EED algorithms will be of three slots. All figures include the theoretical results obtained for 3EED using (3) and (6). For IED, the best theoretical ROC is considered as reference ( $M=L=3$ ) [3]. Monte Carlo simulations were run for CED, 3-OR-CCED, 3-AND-CCED, IED, and 3EED, where CDP and FAP were estimated for 150,000 sensing events. In all simulations, we considered a low signal-to-noise ratio (SNR) of  $SNR = -9.15dB$  as in [3] and that the energy is estimated for  $N = 1000$  signal samples in each sensing event. For 3EED, we used the ideal decision threshold given by (9), while for IED, the threshold is selected according to the conservative approach [3].

In Figure 1, the ROC plots of all algorithms were represented for  $B = 10$  and  $T = 50$ . In this scenario, the PU has a time occupancy of  $B/T = 1/5$ , which is a regular duty cycle value in most of the licensed systems, especially in the uplink [1]. It can be noticed that 3EED performs almost the same as IED and better than CED. Analysing the simulated ROCs, one can see that 3-OR-CCED performs identical to 3EED, while 3-AND-CCED performs worse than CED. This is explained by the fact that 3-OR-CCED is almost identical to 3EED, i.e., the PU signal is detected as present if the energy level exceeds the threshold in any of the three consecutive sensing slots. Also, 3-AND-CCED decides the PU signal as present only if it detects a high energy level in all three slots.

In Figure 2, the algorithms are compared for  $B = 40$  and  $T = 50$ . While for CED and for the theoretical IED, varying the values of  $B$  has no impact on the performance, the other algorithms are affected by this change. When  $B$  increases, it is noticed a decrease of the detection performances for 3-OR-CCED, IED, and 3EED, and a performance increase for 3-AND-CCED. Hence, when increasing the value of  $B$ , we notice that the ROC curve for IED moves downwards, as compared to the theoretical one. This difference is de-

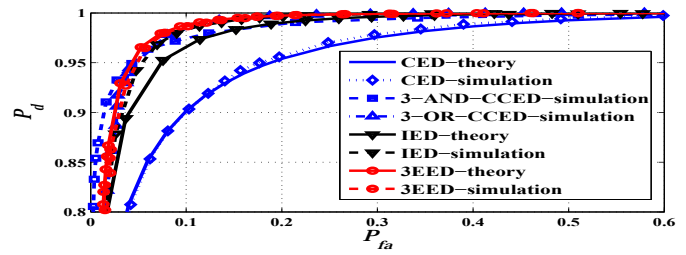


Fig. 3. ROC curves for ED algorithms with  $B = 400$  and  $T = 500$ .

termined by the fact that the IED decision threshold is set similarly to CED (the conservative approach), for a specific target FAP value [3]. This performance depreciation was not noticed in [3], because in all ROC plots, the considered FAP value was the target value, not the experienced (estimated) value. This FAP offset will be analysed in subsection IV-B. Regarding 3EED, its maximum performance is obtained for  $T \gg B \geq 3$ . Nevertheless, for  $T - B \sim 3$ , the performance of 3EED decreases considerably as compared to IED. This depreciation is caused by the fact that all assumptions made in Section III (including setting the threshold in (9)) considered that  $T - B \rightarrow \infty$ . Apparently, this represents a disadvantage, but this scenario ( $B \nearrow T$ ) is not suitable for CR systems, as the available time slots for SU are fewer. Also, the difference between the theoretical and experimental results is smaller for 3EED when compared to IED, confirming the assumptions made in Section III. In conclusion, 3EED performs the same as IED for  $T - B \gg 3$  and shows a smaller difference between theoretical and experimental results. For the CCED algorithms, we notice in Figures 1 and 2 that 3-OR-CCED performs almost the same as 3EED, for any value of  $B$ , while the performance of 3-AND-CCED is improved when  $B$  increases. The performance improvement for 3-AND-CCED is explained by the fact that for large values of  $B$ , there are more groups of three consecutive slots where the PU signal is present.

Similar results are depicted in Figure 3 for  $B = 400$  and  $T = 500$ . Comparing Figures 2 and 3, one can notice that when the values of  $B$  and  $T$  increase by the same factor, the performance of 3EED is improved as compared to IED. Nevertheless, the performances of all algorithms (excepting CED) are improved. This performance increase for 3EED is explained by the fact that any increase in the number of sensing events (for the same  $B/T$  value) will allow a more accurate detection of the transitions from "idle" to "busy" and vice versa. Hence, if the condition  $T - B \gg 3$  is met, the ROC performance can be increased even for a high duty cycle, but this solution is computationally expensive, because it requires a higher number of sensing events per time unit. For  $T = 500$ , the IED performance is also improved as compared to  $T = 50$ . In fact, the theoretical ROC limit (the same in Figures 1-3, with  $M=L=3$ ) is exceeded by the simulation results in Figure 3. This performance increase can be explained by the fact that IED is also dependent on the PU duty cycle and this needs further investigation. Also, excepting CED, all algorithms perform almost the same.

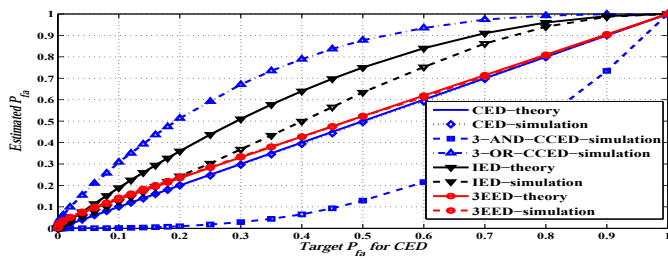


Fig. 4. FAP offset for ED algorithms ( $B = 10, T = 50$ ).

### B. Offset analysis for target FAP and CDP

As mentioned in subsection IV-A, the FAP values determined for each algorithm show an offset when compared to the corresponding target FAP value of CED. Actually, both IED and 3EED algorithms combine CED detections from different slots. For example, according to equation (24) in [3], a target FAP is selected for IED, but the experienced FAP is always larger than the target value, when a conservative approach is considered. Hence, this estimation introduces an offset between the target and the experienced performances. On the other hand, for 3EED we developed an exact expression of the decision threshold, given by (9). In order to study the accuracy of the FAP estimation, we propose a different graphical representation. In Figure 4, the experienced FAP values are represented as a function of the target FAP values selected for CED. Obviously, representing the estimated FAP as a function of the target FAP for CED introduces the identity function in this graph. It is important to note that the FAP plot for 3EED is the closest one to the identity function. The estimated FAP values for IED are larger than for 3EED, corresponding to the same target FAP values of CED. Moreover, the simulation FAP values are smaller than the theoretical ones for IED. Regarding the CCED algorithms, even larger offsets between the estimated FAP and the corresponding target FAP values were noticed. Even if the results presented in Figure 4 are estimated for the particular values of  $B = 10$  and  $T = 50$ , we obtained similar plots for different values of  $B$  and  $T$ . In conclusion, even if the ROC plots from Figures 1-3 show similar performances for IED, 3-OR-CCED, and 3EED, the latter presents a smaller FAP offset. Therefore, for the other algorithms, excepting 3EED, it is more difficult to impose a specific ROC point as a practical operating regime.

### C. Computational complexity analysis

In Table I, the complexity of the considered ED algorithms is compared by estimating the number of required elementary math and logical operations, such as: multiplications ( $\times$ ), additions ( $+$ ), divisions ( $\div$ ), and comparisons ( $\geq$ ). Also, the memory locations necessary to save  $E_i$  or  $q_i$  values (other than the current; noted as 'Mem.') and the delay (in number of sensing slots; noted as 'D.') are evaluated. For all algorithms,  $N$  is the number of signal samples from one sensing slot. All algorithms have an increased complexity as compared to CED. For example, IED needs more  $L - 1$  additions and 1 division to estimate the average energy, 2 more comparisons, and occupies  $L - 1$  memory locations to save previous  $E_i$

TABLE I  
COMPUTATIONAL COMPLEXITY ANALYSIS FOR ED ALGORITHMS

Alg.	$\times$	$+$	$\div$	AND	OR	$\geq$	Mem.	D.
CED	$N$	$N - 1$	0	0	0	1	0	1
IED	$N$	$N + L - 2$	1	0	0	3	$L - 1$	1
3EED	$N$	$N - 1$	0	0	0	3	2	2
3AND	$N$	$N - 1$	0	2	0	1	2	1
3OR	$N$	$N - 1$	0	0	2	1	2	1

values. Also, 3EED needs 2 more comparisons, occupies 2 memory locations to save the  $E_i$  values, and introduces an additional delay of maximum 1 slot. For IED and 3EED, the complexity is calculated for the worst-case scenario, when all three decisions are required. Finally, each CCED algorithm uses 2 more 2-input logical operations ("AND" and "OR") and occupies 2 memory locations to save previous  $q_i$  values. We can notice that the complexity of IED is higher than 3EED's. In previous subsections, for the sake of comparison fairness, but also, for a good compromise between complexity and performance (according to [3], for  $L > 3$  there is no significant IED performance improvement), the value of  $L$  is fixed to 3. In this case, IED needs a supplement of 2 additions and 1 division, and it does not need additional memory, as compared to 3EED. However, 3EED introduces an additional delay of maximum 1 slot, which represents its only disadvantage. Despite these complexity differences, the total operating time is approximately the same for all algorithms due to the high-speed hardware used in all current applications.

### V. CONCLUSION

In this work, we introduced a new ED algorithm, named 3EED, and compared its performance and complexity with other ED algorithms. 3EED offers a good detection performance, a low complexity and the smallest FAP offset. As future research goals, we aim to extend the analysis of 3EED for more complex PU activity models and channel types, to quantify its robustness with respect to PU's activity variation, and to test its performance in real CR systems.

### REFERENCES

- [1] M. Lopez-Benitez and F. Casadevall, "Spectrum Occupancy in Realistic Scenarios and Duty Cycle Model for Cognitive Radio," *Advances in Electronics and Telecommun., Special Issue on Radio Commun.*, vol. 1, no. 1, pp. 26–34, Apr. 2010.
- [2] H. Urkowitz, "Energy detection of unknown deterministic signals," *Proceedings of the IEEE*, vol. 55, no. 4, pp. 523–531, Apr. 1967.
- [3] M. Lopez-Benitez and F. Casadevall, "Improved energy detection spectrum sensing for cognitive radio," *IET Commun., Special Issue on Cognitive Commun.*, vol. 6, no. 8, pp. 785–796, May 2012.
- [4] S. Akin and M. C. Gursoy, "Performance Analysis of Cognitive Radio Systems under QoS Constraints and Channel Uncertainty," *IEEE Trans. Wireless Commun.*, vol. 10, no. 9, pp. 2883–2895, Sept. 2011.
- [5] X. Ling et al., "Adaptive Threshold Control for Energy Detection Based Spectrum Sensing in Cognitive Radios," *IEEE Wireless Commun. Lett.*, vol. 1, no. 5, pp.448–451, Oct. 2012.
- [6] F. Gaaloul et al., "Switch Based Opportunistic Spectrum Access for General Primary User Traffic Model," *IEEE Wireless Commun. Lett.*, vol. 1, no. 5, pp. 424–427, Oct. 2012.
- [7] K. W. Choi and E. Hossain, "Estimation of primary user parameters in cognitive radio systems via hidden Markov model," *IEEE Trans. Signal Process.*, vol. 61, no. 3, pp. 782–795, Mar. 2013.
- [8] K. Haghighi, E. G. Ström, and E. Agrell, "Sensing or Transmission: Causal Cognitive Radio Strategies with Censorship," *IEEE Trans. Wireless Commun.*, vol. 13, no. 6, pp. 3031–3041, June 2014.